Simulated 2n Efficiency in ST-mona

Michael D. Jones

Aril 6 2012

1.0 Efficiency

Simulations of ^{14}Be$\rightarrow^{13}$Li$^{*}\rightarrow^{11}$Li+2n were performed in ST-mona over a range of beam energies from 55 – 300 MeV/u in incriments of 50 MeV/u with a flat input decay energy distribution:

```
arguments="-exp 05034_Be -geant -reac 2neutron  -e uniform 0.05 10
           -e1 const 0.01 -n ### -strag 1 -glaub 1.0 -be ###"
```

Where "–e uniform 0.05 10" fixes the total decay energy to be constant between 0.05 – 10 MeV, and "–e1 const 0.01" sets a lower bound on the decay energy of the first neutron in the sequential decay. The neutron energies are then randomly sampled from this flat distribution.

Each simulation was run at n = 200,000 [1]. The input decay spectrum was reconstructed with the alias:

```
tg->SetAlias("Input3body","b2p0R_exen + b2p0R_exen2");
```

This sums the energies of the two neutrons. The simulated decay spectrum was then obtained by gating on the multiplicity, relative distance and velocity:

```
Multiplicity:
tg->SetAlias("good_mult","b13pn1gmultiplicity + b13pn2gmultiplicity");

Causality Cuts:
tg->SetAlias("gRHO_01","100*TMath::Sqrt(
               TMath::Power(b13pg1x-b13pg2x,2.0)
              +TMath::Power(b13pg1y-b13pg2y,2.0)
              +TMath::Power(b13pg1z-b13pg2z,2.0))");

tg->SetAlias("gVREL_01","gRHO_01/(b13pg2t-b13pg1t)");
```

[1] Except for 300 MeV/u where n = 50,000 due to space limitations. EDITED:5/7/12 Re-ran simulation and corrected figrues

Where gRHO_01 is the distance between the two neutrons in a MoNA bar:

$$\rho = \sqrt{(x_1 - x_2)^2 + (y_1 - y_2)^2 + (z_1 - z_2)^2} \tag{1}$$

And gVREL_01 is the relative velocity:

$$v_{rel} = \frac{\rho}{t_2 - t_1} \tag{2}$$

The g2nCut gate is then defined:

```
tg->SetAlias("g2nCut1","gRHO_01>30 && gVREL_01>11");// [cm/ns]
```

Here the cuts are placed at $\rho > 30$ [cm] and $v_{rel} > 11$ [cm/ns]. The velocity cut for a given beam energy was estimated assuming the beam was non-relativistic:

$$E_{beam} * n_{nucleon} = \frac{1}{2} M_{Be} v^2 \;\rightarrow\; v_{beam} = \sqrt{\frac{2E_b * n_n}{M_{Be}}}$$

Plotting the Input3body alias with gates on multiplicity and 2n cuts gives a spectrum proportional to the efficiency as a function of decay energy. Dividing by the un-gated Input3Body histogram then yields the efficiency curve:

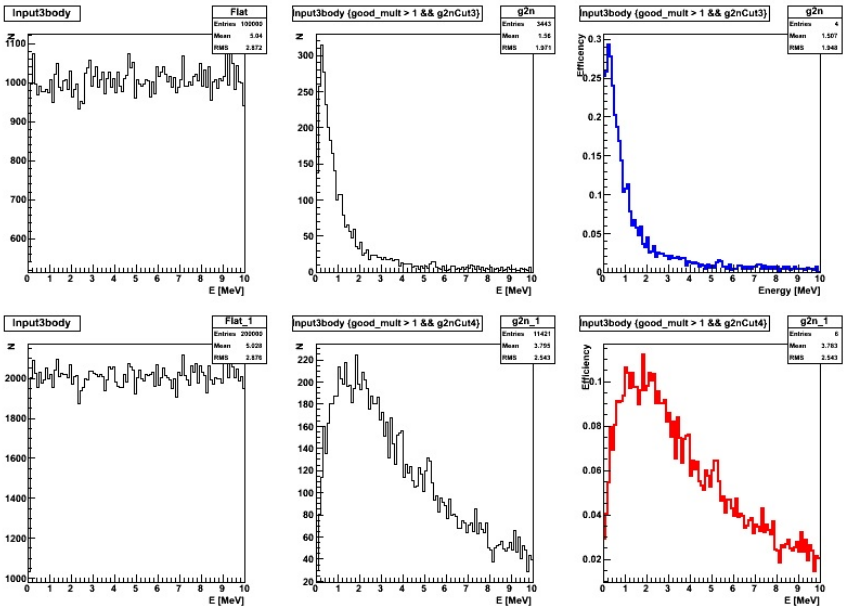

Figure 1: Comparison of Input3Body with and without cuts. The top row is a simulation at 55 MeV, and the bottom at 300 MeV. The efficiency (%) is shown in the rightmost graphs.

To determine proper distance and velocity cuts contour plots of v_{rel} vs. ρ were made with multiplicity and true2n cuts. The true2n gate was defined as:

```
tg->SetAlias("true2n", "(b13pg1x == b13pn1g1x && b13pg2x == b13pn2g1x)
    ||  (b13pg1x == b13pn2g1x  &&  b13pg2x == b13pn1g1x)");
```

Which demands that the x-position of the two neutrons originate from the same location. No condition was placed on the y and z positions. Phase space plots for 55 MeV and 300 MeV with gates on multiplicity, true2n and false2n (!true2n) are shown below:

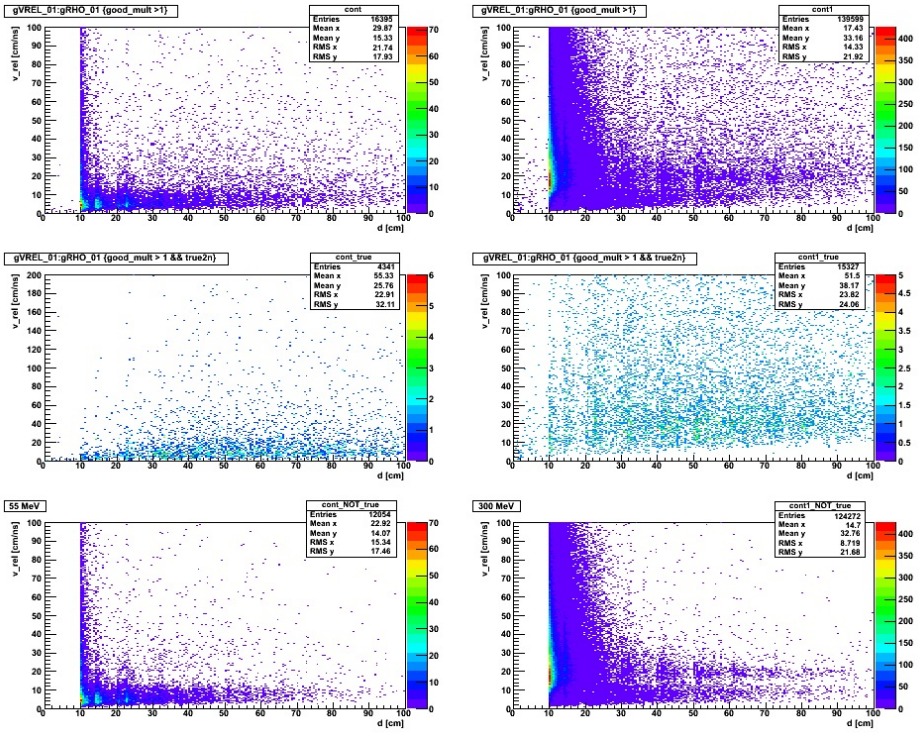

Figure 2: Plots of phase space for 55 MeV (left) and 300 MeV (right). v_{rel} [cm/ns] is on the Y-axis, and ρ [cm] on the X-axis. From top to bottom, the applied cuts are: good_mult $>$ 1, good_mult $>$ 1 && true2n, and good_mult $>$ 1 && !true2n.

Most notable is the complete shift in the concentration of false 2n events between 55 and 300 MeV/u. At lower energies most of the false events are restricted to low velocities but extend to $\sim$50 [cm], while at 300 MeV/u a majority of the false events are restricted to small distances but extend to higher velocities.

To see where the false 2n events lie over the range of simulated energies, phase space diagrams were made for each simulation:

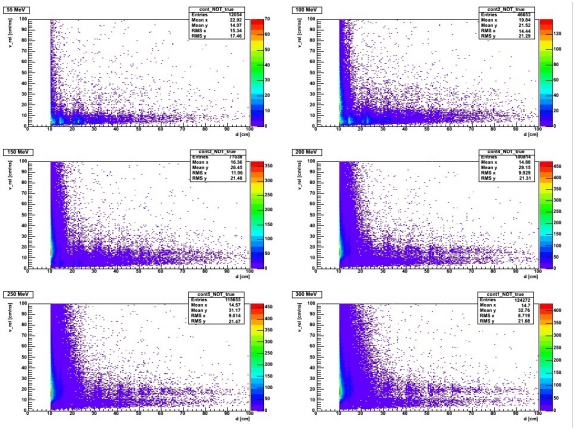

Figure 3: False 2n plots for sampled beam energies with a !true2n gate. Left to right: 55 $\rightarrow$ 300 MeV in incriments of 50 MeV.

Placing a distance cut at 30 [cm] and v_{rel} at beam velocity, the efficiency was calculated for each energy:

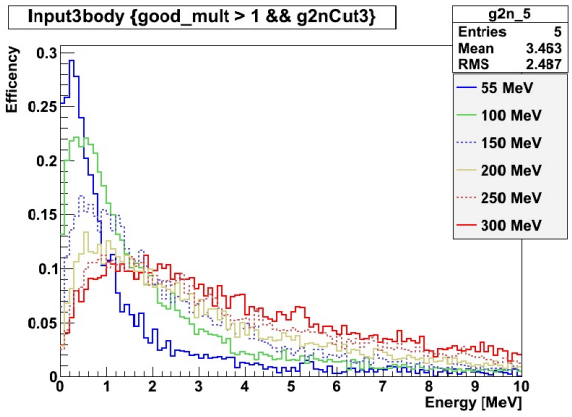

Figure 4: Simulated efficiency (%) of decay energy for the sampled beam energies.

Here we see that as the beam energy increases, the efficiency for low decay energies (< 1 MeV) begins to drop dramatically. In addition, As E_{beam} increases, the efficiency curve begins to peak at higher decay energies. However, between 55 and 300 MeV the overall magnitude of the peak is reduced by a factor of ~ 3.

1.1 True Efficiency

Examining the False2n plot (Figure 3) we see that false 2n events are included in our distance and velocity cuts. Thus it is neccessary to calculate the percent of false events within our 2n cut, for it is possible that at higher energies many more false events are included in the efficiency curve. This would cause the calculated efficiency to not give an accurate representation of the true 2n efficiency. To determine the fraction of true events within the 2n cut, g2nCut and true2n gates were applied to the Input3body spectrum and the ratio: $\%True = (True2n \wedge g2nCut)/g2nCut$ was taken to determine the % of true 2n events in the 2n cut. This was accomplished in ROOT by dividing the two histograms.

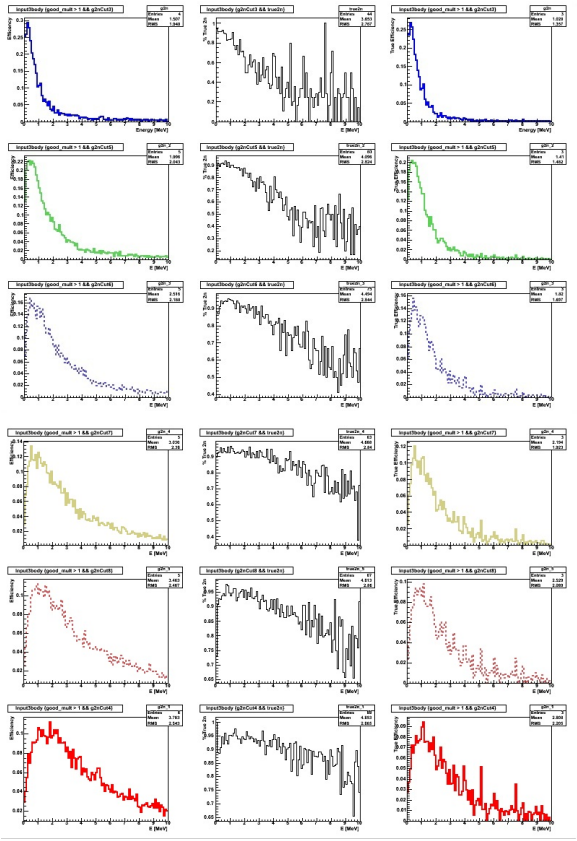

Figure 5: Top to Bottom is increasing energy from 55–300 MeV. Left: Efficiency with dstance and v_{beam} cuts. Middle: %True 2n events in g2nCut gate. Right: Efficiency folded with %True2n.

A plot of the efficiency before and after is shown below to illustrate the %True2n correction:

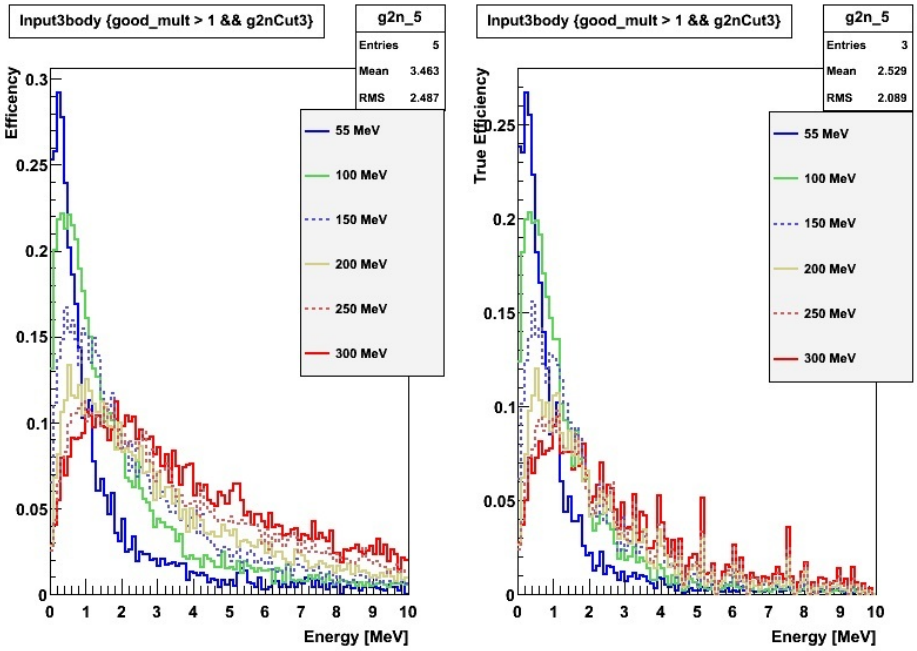

Figure 6: Left: efficiency curves before folding with %True2n. Right: efficiency after folding.

1.2 Conclusion

The simulated 2n efficiency of MoNA begins to decrease rapidly for lower decay energies as the beam velocity is increased. At the same time however, there is a slight increase in efficiency for decay energies above 1 MeV. This gain in efficiency at higher decay energies comes at the cost of lower energies, which may be useful if the lower decay energies are undesired. For example, at 2 MeV, the gain in efficiency between 55 and 100 MeV/u is approximatly a factor of 2, and if one can afford to sacrifice efficiency for energies in the keV range, then it would be advantageous to move to a higher beam energy. It is important to note that in these simulations, due to a lack of data beyond 150 MeV, the cross-section data had to be extrapolated which introduces a large degree of uncertainty that could potentially change the shapes of these efficiency curves dramatically.

2.0 Comparison between 55 and 300 MeV

The simulation was repeated at 55 and 300 MeV/u with a breit wigner energy distribution:

```
arguments="-exp 05034_Be -geant -reac 2neutron  -e1 bw 0.5 0.2
          -e2 bw 0.2 0.05  -n ### -strag 1 -glaub 1.0 -be ###"
```

$$f(E; E_0, \Gamma) = \frac{1}{\pi} \frac{\Gamma/2}{(E - E_0)^2 + \Gamma^2/4}$$

Which sets the decay energy of each neutron as a breit wigner distribution with widths and centers $E_0^{(1)} = 0.5$ [MeV], $\Gamma^{(1)} = 0.2$ [MeV], and $E_0^{(2)} = 0.2$ [MeV], $\Gamma^{(2)} = 0.05$ [MeV] respectively. The multiplicity distributions of the two simulations are shown below:

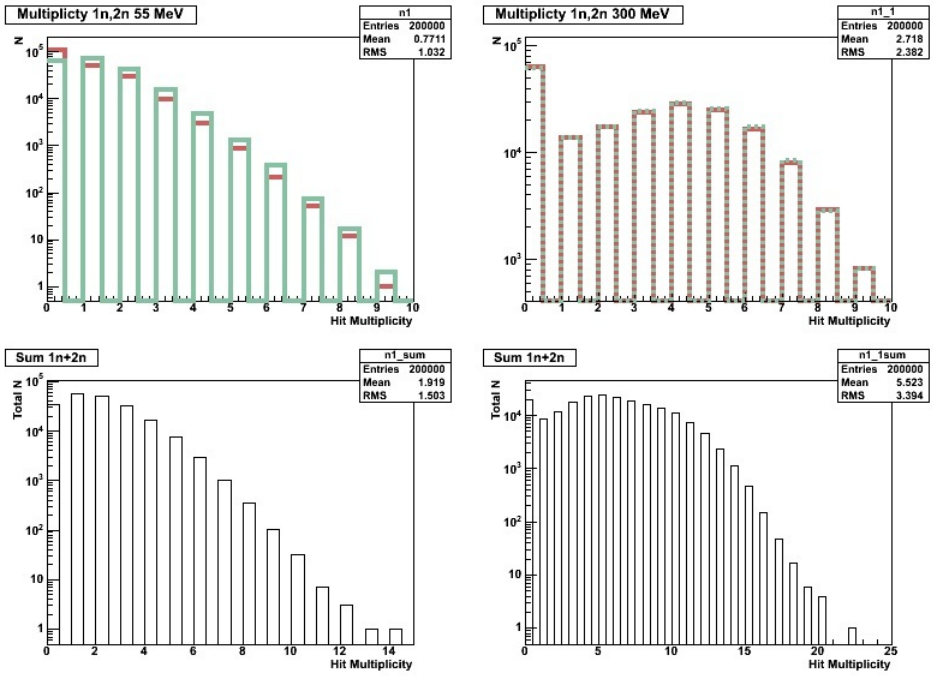

Figure 7: Comparison of 2n multiplicity distributions (good_mult) between 55 (left) and 300 MeV/u (right). Red and green represent the individual multiplicity of the first and second nuetron respectively. The total 2n multiplicity is on the bottom in log scale.

The total energy deposited and light output in the PMT was determined with the aliases:

```
tg->SetAlias("Lsum","b13pg1light+b13pg2light+...+b13pg20light");
tg->SetAlias("Esum","b13pg1Edep+b13pg2Edep+...+13pg20Edep");
```

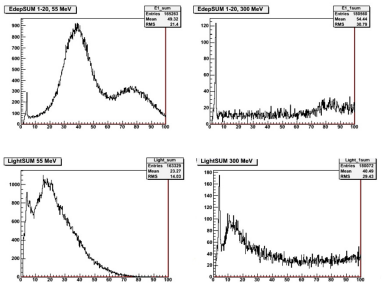

Figure 8: Plots of total energy deposited (MeV) and light output (meVee) for 55 and 300 MeV/u. A gate was placed on $E_{sum} > 1.5$ [MeV] and Lsum > 1.5 [meVee] due to an intense low lying peak that washes out much of the structure.

Between 55 and 300 MeV/u the shape of these spectra change dramatically. The "double-hump" in the E_{dep} is lost completely at 300 MeV/u, It would appear that only the low energy peak at ~ 5 MeV remains, with the distribution being mostly flat. Similarly, at higher energies, the overall magnitude of the light output is significantly reduced and the tail is extened much further. This is reflected in the reduced efficiency at higher energies (Figure 6).

Contour plots of multiplicity vs. light output were also made to examine the dominant contribution to the light output:

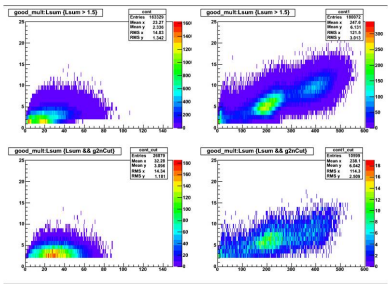

Figure 9: Contour plots of multiplicity vs. light output [meVee] for 55 and 300 MeV/u. In the top graphs, there is a cut on Lsum > 1.5 [meVee] to resolve the structure. In the bottom graphs, both Lsum > 1.5 [meVee] and a 2n gate are applied.

As seen by applying a 2n cut, a majority of the light output comes from false 2n events by an order of magnitude. Of the true2n events many of them are of

multiplicity < 5 at 55 MeV/u. However at 300 MeV/u much of the light output comes from 2n events with multiplicity $4 < g < 8$. In addition to extending to higher mulitplicities and light outputs, additional areas of concentrated events appear at 300 MeV/u. There are 3 distinct areas of intensity in the upper right graph which become hard to resolve once the cut is applied due to low statistics.